A New Grid-Based Monte-Carlo Code for Raman Scattered He II : Preliminary Results

Bo-Eun Choi, Seok-Jun Chang, Hee-Won Lee
Department of Physics and Astronomy, Sejong University

1. Introduction

Raman He II Features in Symbiotic Stars and Planetary Nebulae

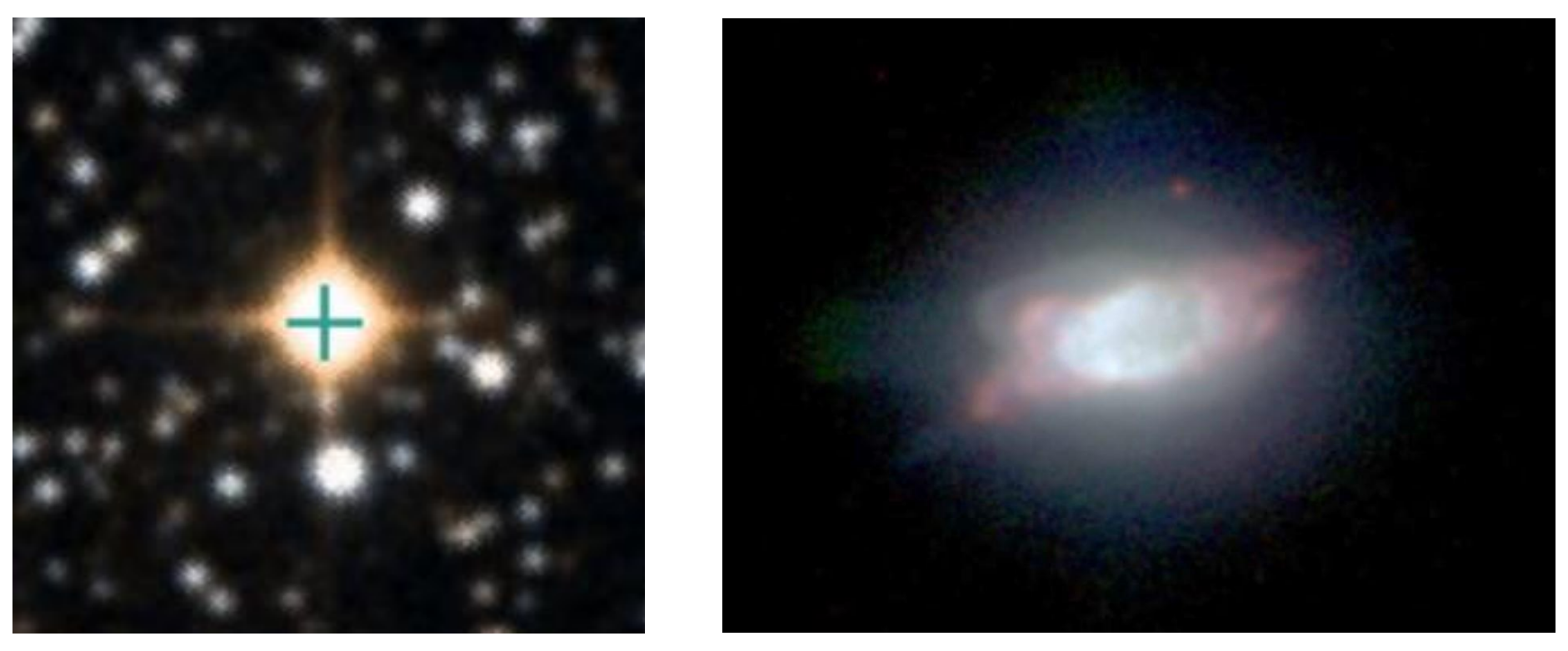

Figure 1. Symbiotic star V1016 Cyg(left) and HST image of young planetary nebula IC 5117(right).

- Symbiotic stars are wide binary systems of a hot white dwarf and a mass-losing giant.
- Young planetary nebulae with a hot central star are surrounded by an H I region associated with the heavy mass-loss at the giant stage.
- When He II UV photons are incident on the thick H I region, they can be transferred via Raman scattering.
  → **hot emission + thick H I region**

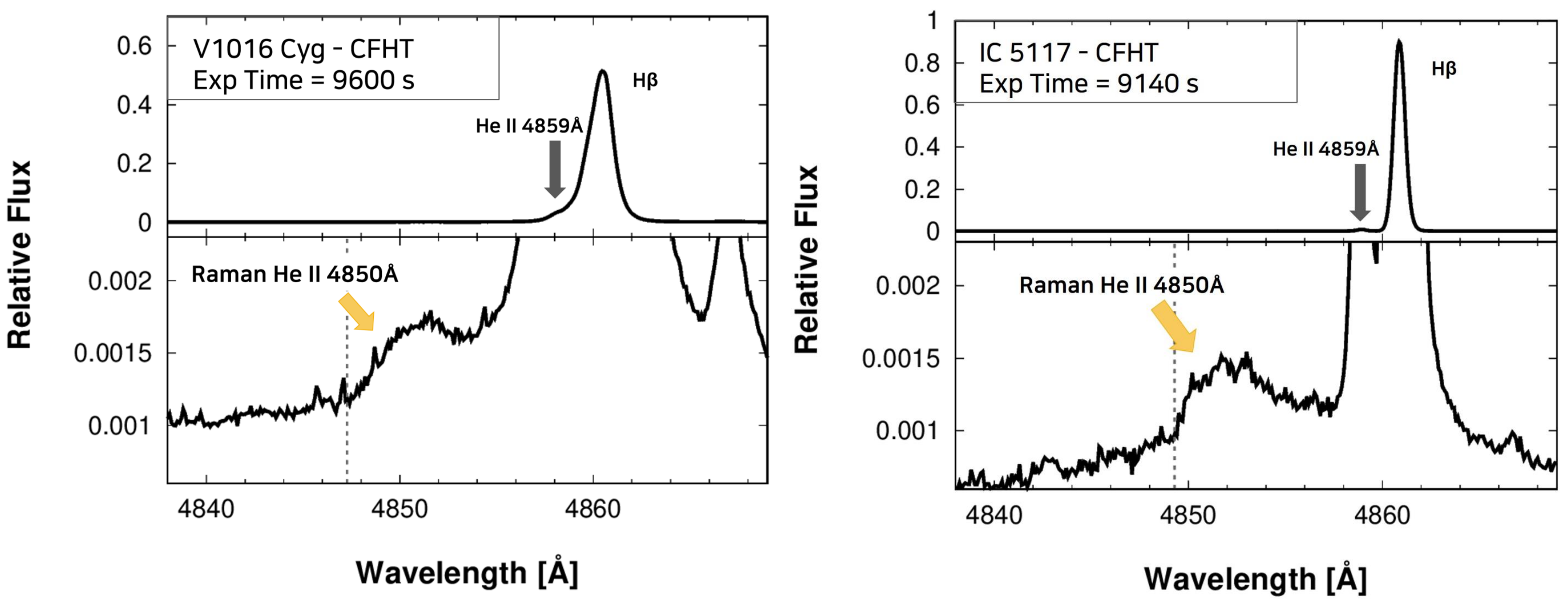

Figure 2. CFHT spectra of V1016 Cyg and IC 5117 around Raman He II 4850.

- Red-shifted Raman scattered He II lines and nearby He II emission lines.

Raman scattered He II

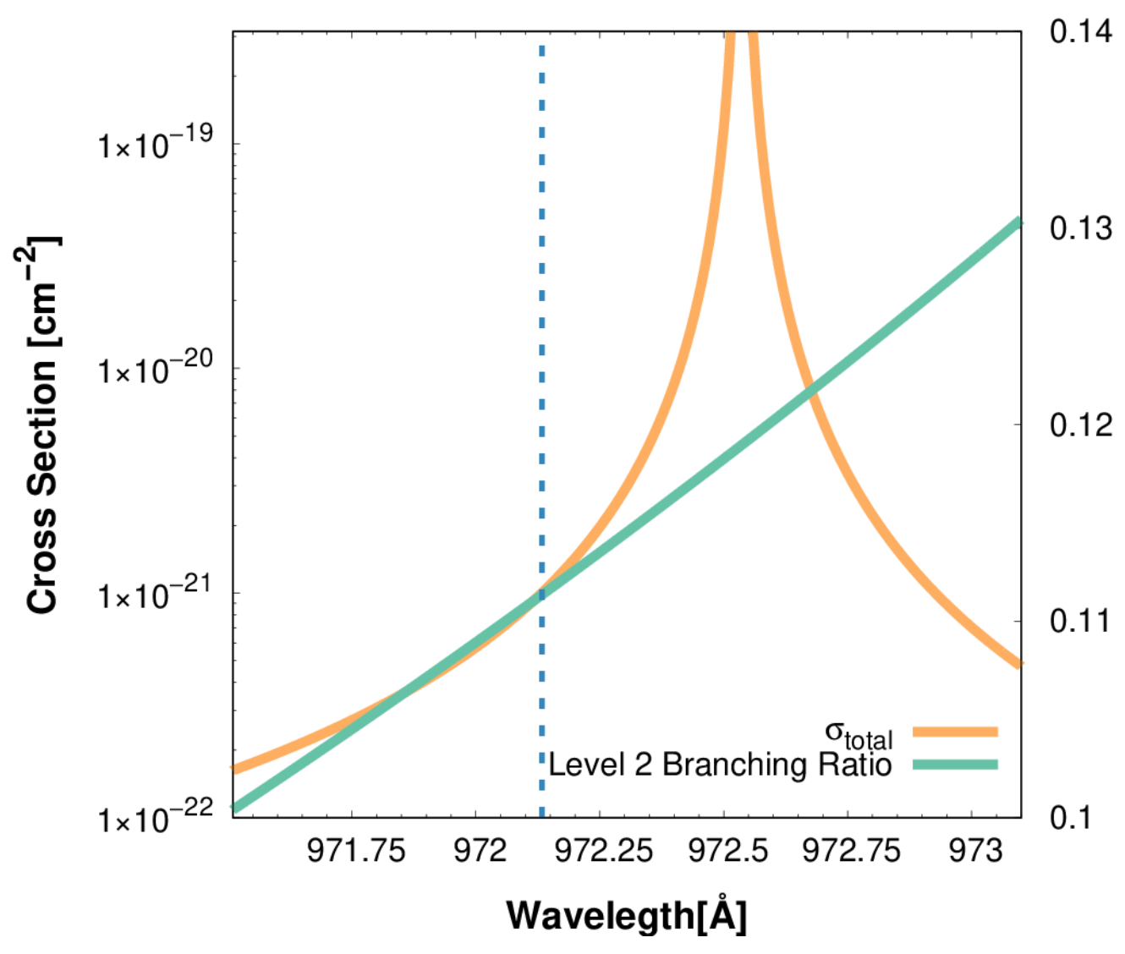

- The cross section increases sharply near resonance.
- Inelastic collision $E_f = E_i - E_{Ly\alpha}$
- Line broadening

$$\frac{1}{\lambda_f} = \frac{1}{\lambda_i} - \frac{1}{Ly\alpha} \Rightarrow \frac{\Delta\lambda_f}{\lambda_f} = \left(\frac{\lambda_f}{\lambda_i}\right)\frac{\Delta\lambda_i}{\lambda_i}$$

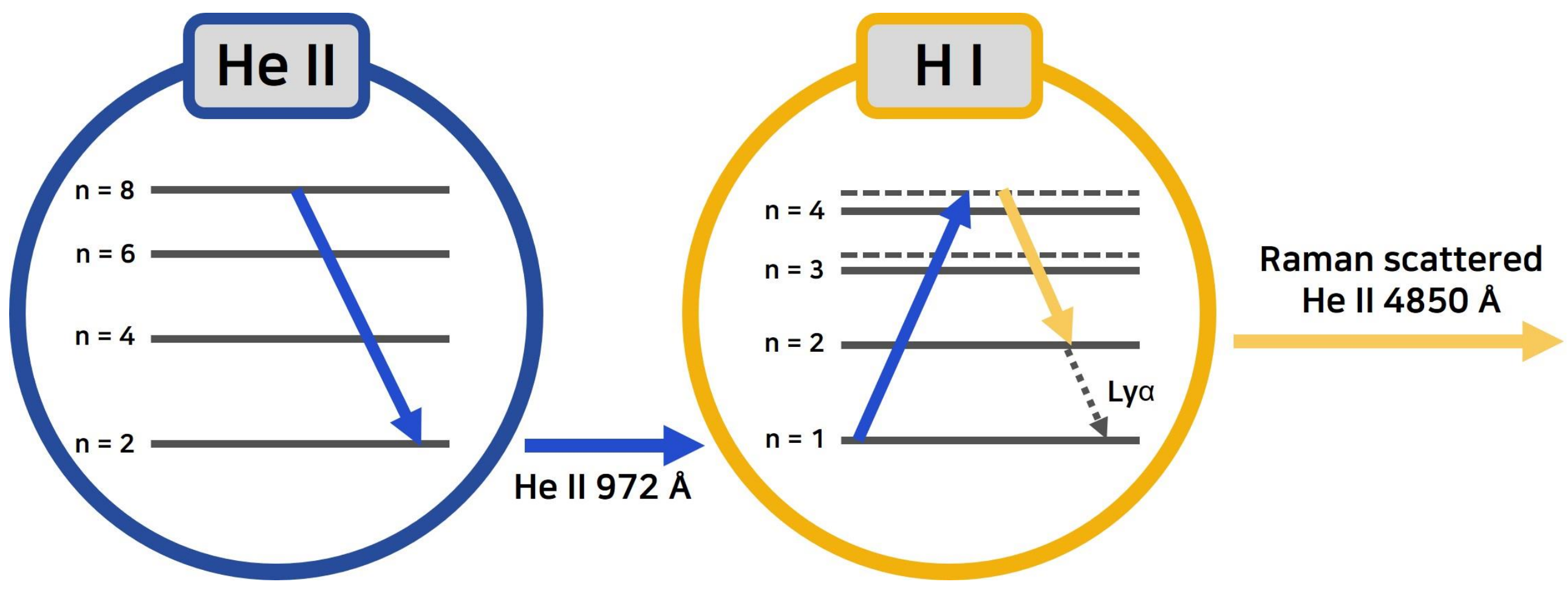

Figure 3. Cross section of HI near Lyγ and the branching ratio of transition to level 2
Figure 4. A schematic illustration of Raman scattering processes

2. Grid-based Numerical Radiative Transfer

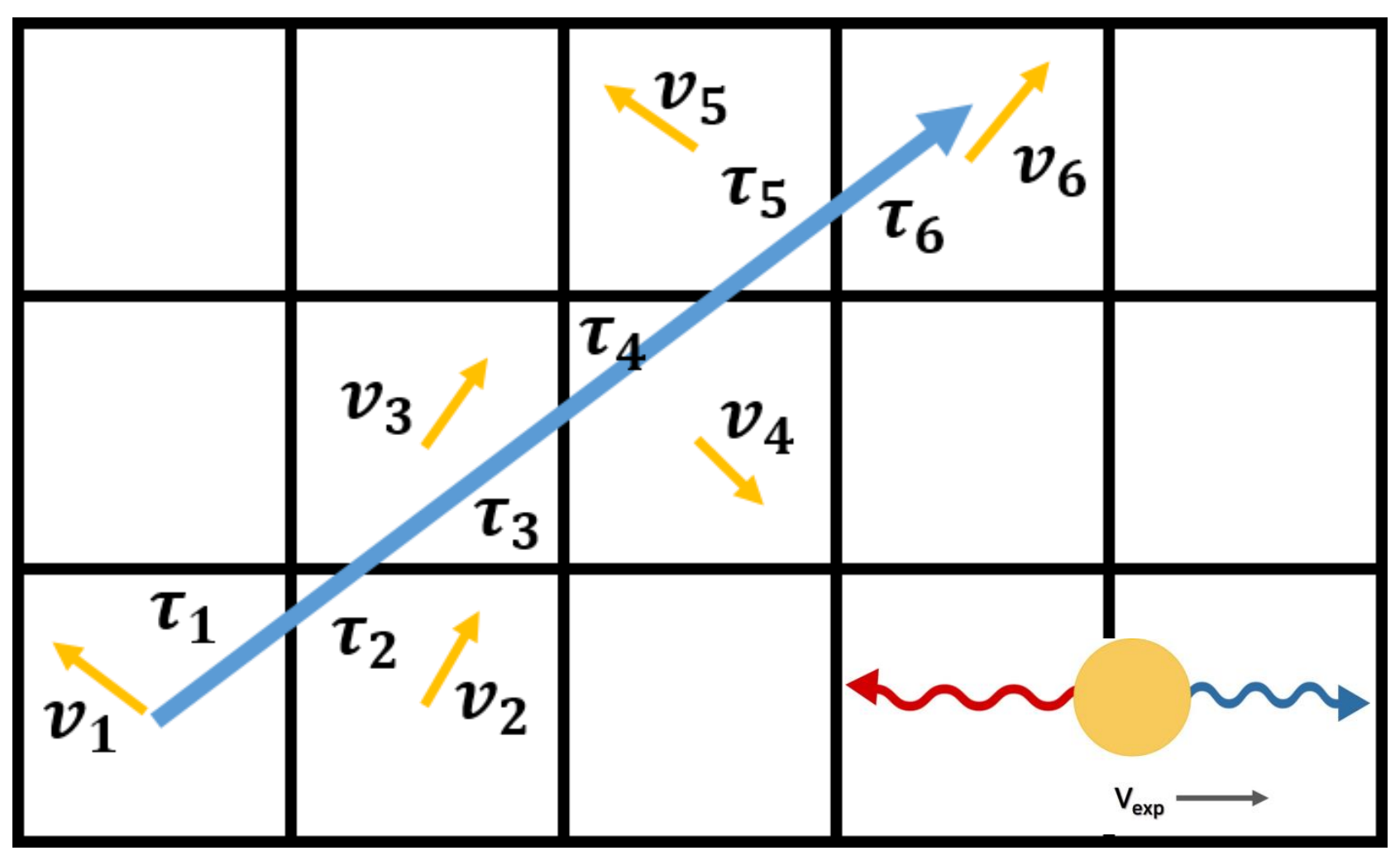

Figure 5. Optical depth of a ray passing through 6 grids. As each grid is moving, the photon frequency in the grid rest frame varies.

- A grid-based approach is necessary to incorporate the kinematics and density distribution of the scattering region.

$$\tau = \tau_1 + \tau_2 + \tau_3 + \tau_4 + \tau_5 + \tau_6$$

- The optical depth for each grid is computed with the cross section for the photon wavelength in the grid rest frame.
- In each grid, the physical conditions are taken to be uniform.

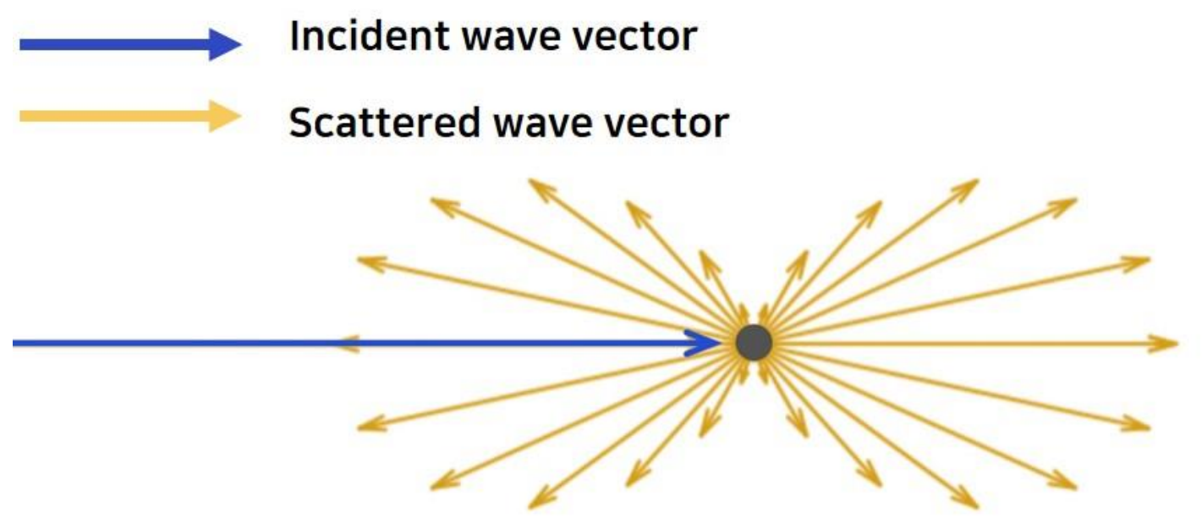

Figure 6. Phase function of scattering.

3. Geometry of Radiative Transfer

- Assume a monochromatic He II emission source is surrounded by a spherical shell-like H I region.
- He II UV photons can escape the scattering region by Rayleigh and Raman scattering.
- The H I region is moving away from the He II source with constant velocity v$_{exp}$.

- Parameters
  - **N$_{HI}$** (column density)
  - **v$_{exp}$** (expansion velocity of the HI region)

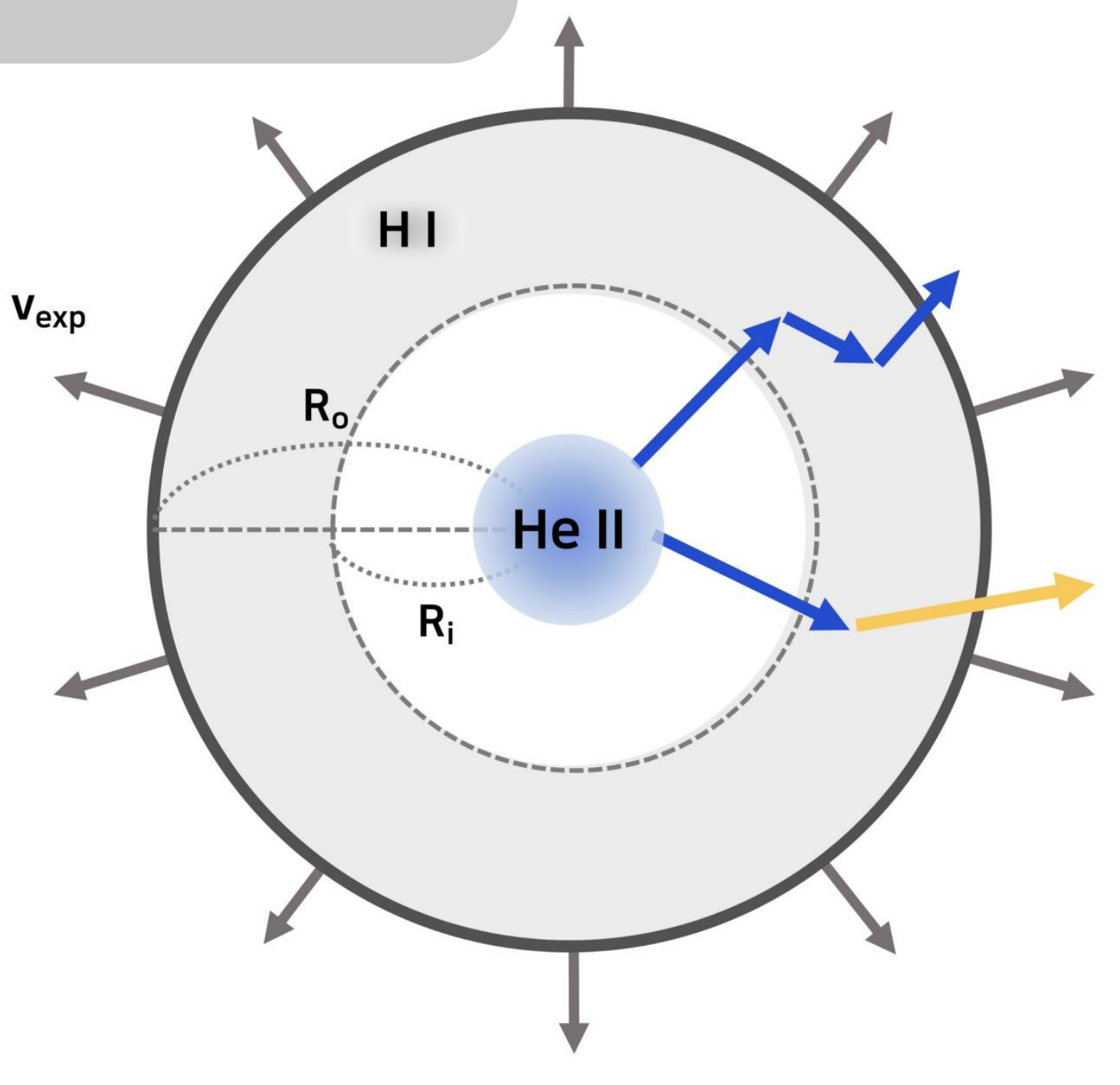

Figure 7. Scattering geometry consisting of a point-like monochromatic He II source surrounded by a neutral spherical shell. The H I number density is determined by geometrical parameters R$_i$ and R$_o$ and physical parameter N$_{HI}$

4. Results

Raman He II Profiles

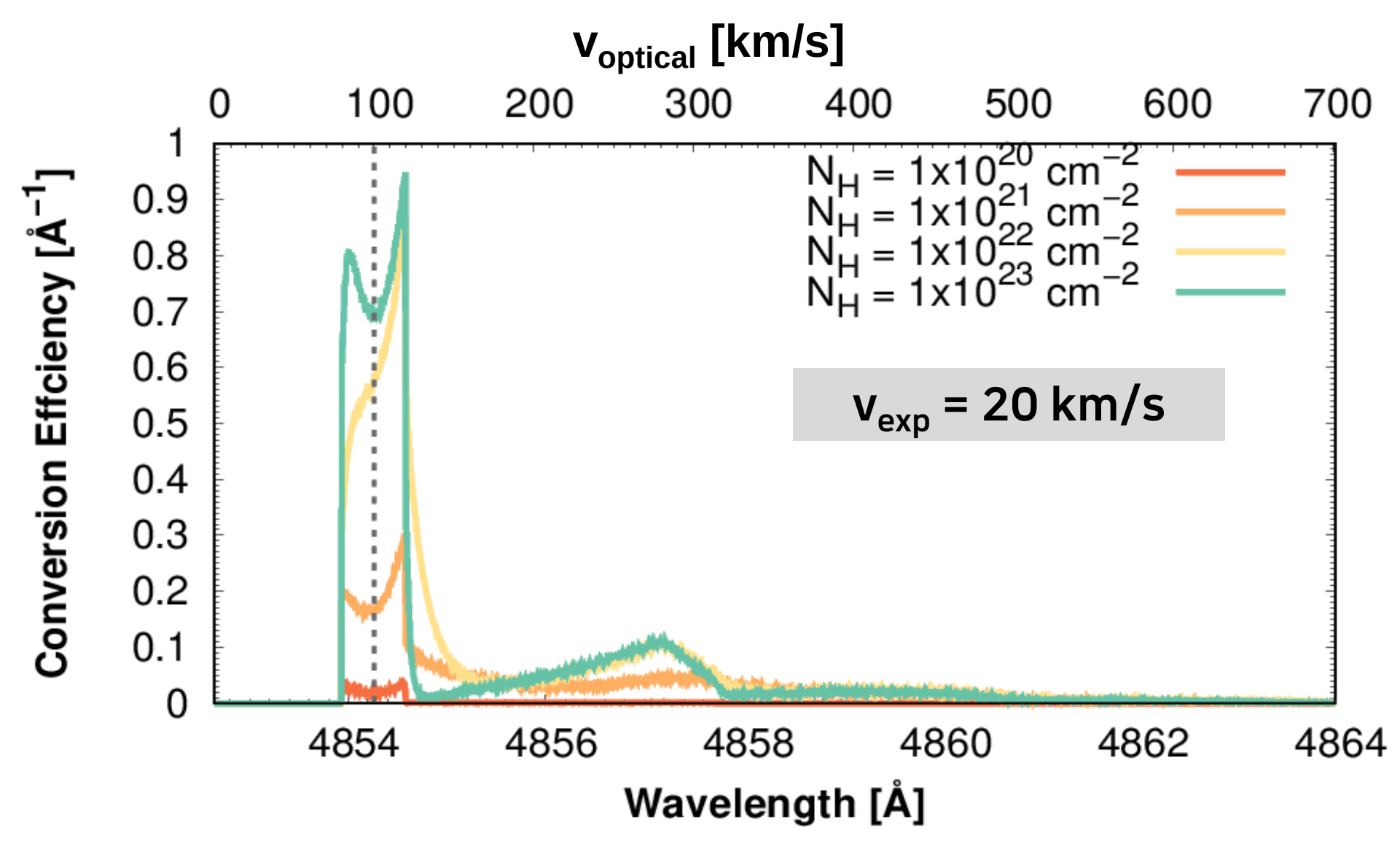

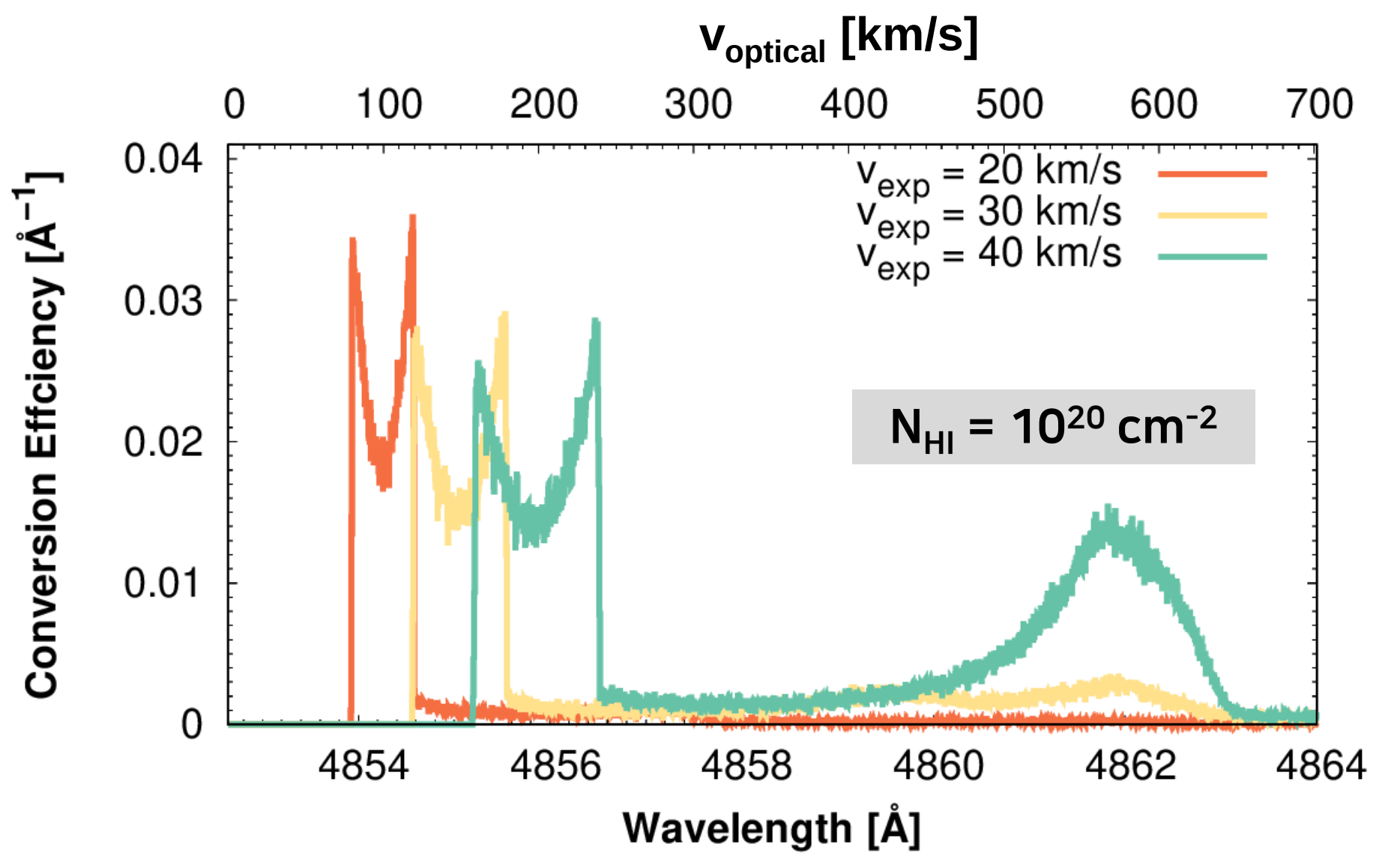

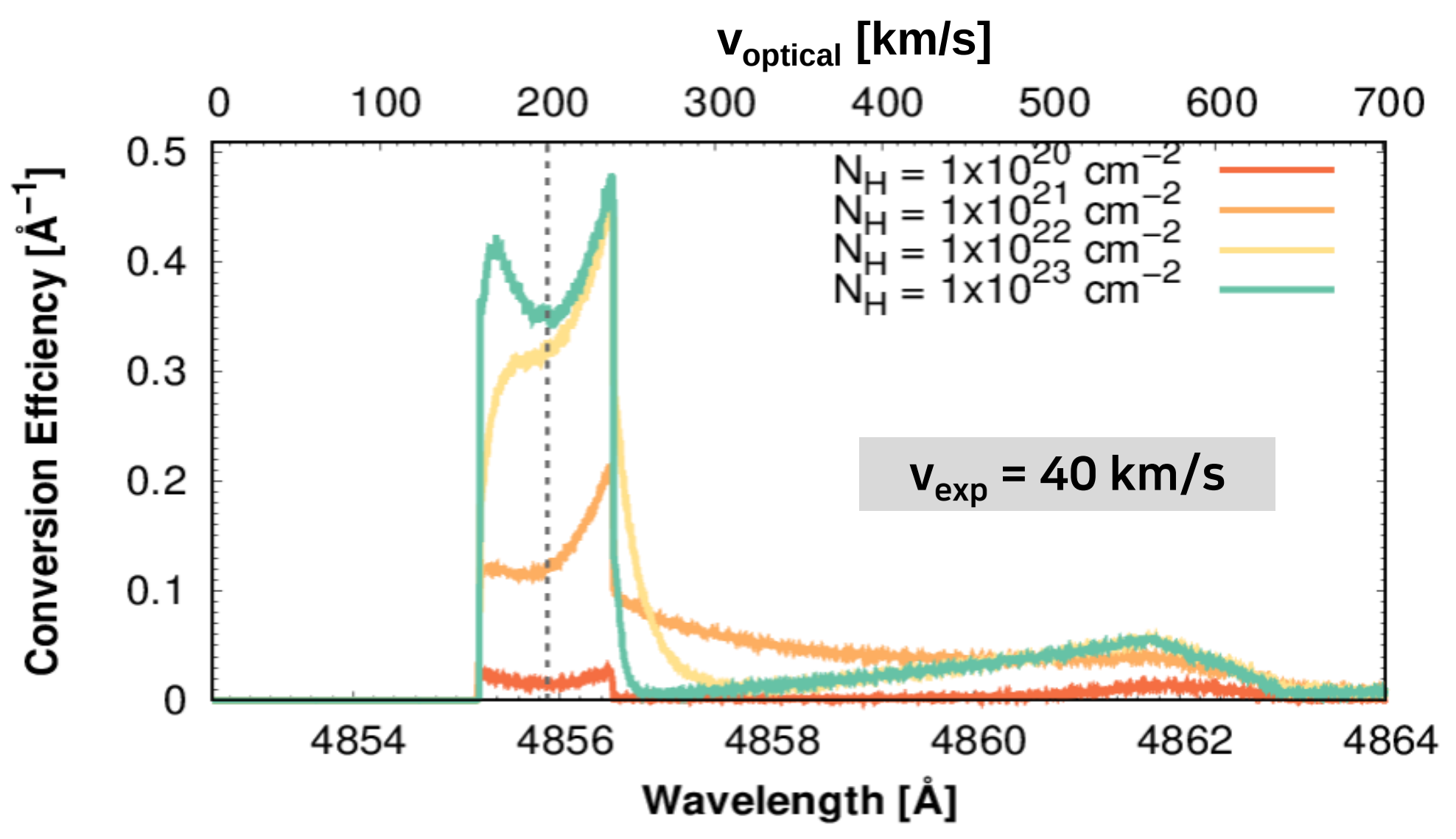

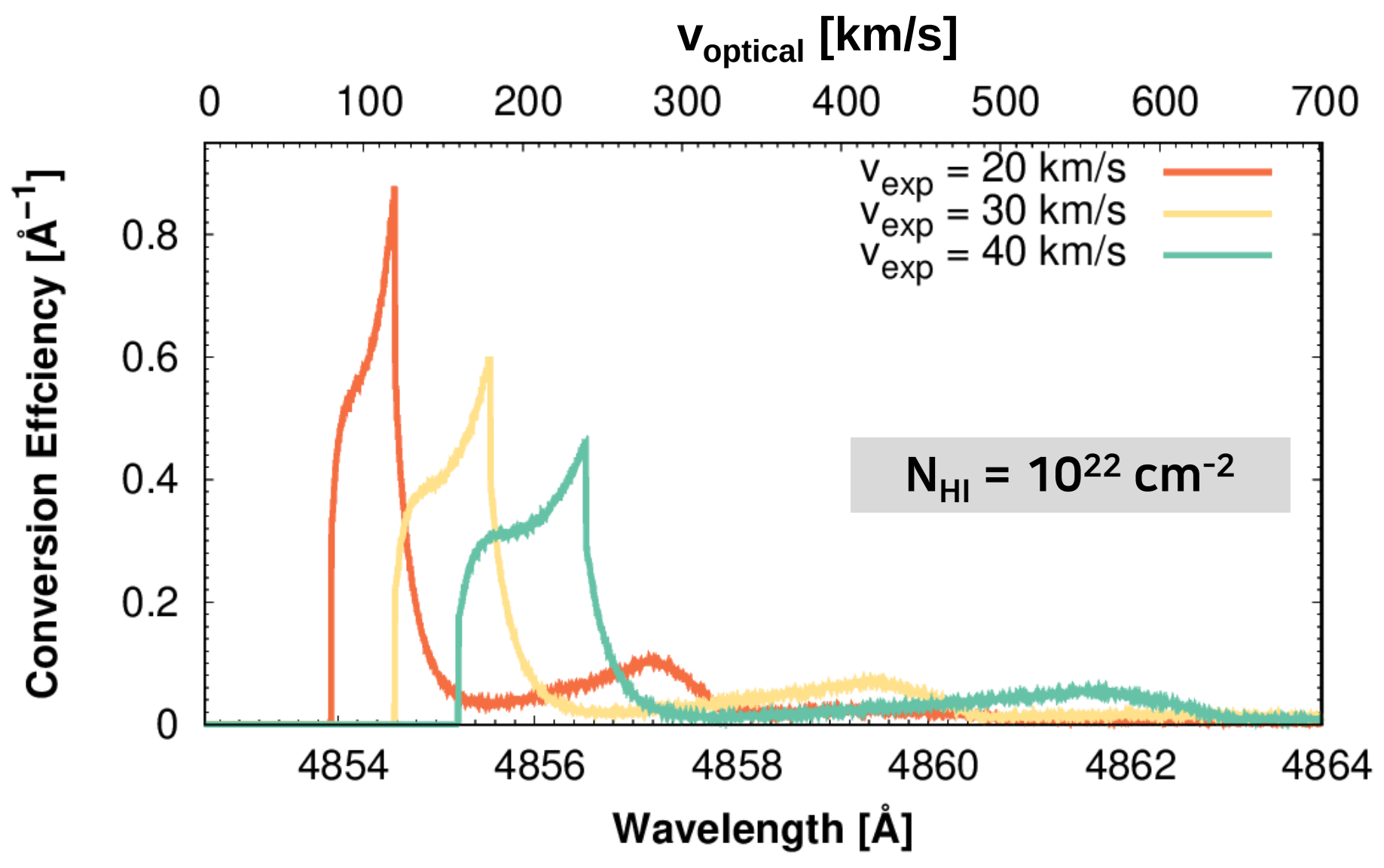

- In the left two panels we show the resultant Raman He II profiles for various HI column densities and the two values 20 km/s and 40 km/s of the expansion velocity of the HI region.
- The two right panels show the resultant Raman He II profiles for various expansion velocities and the two HI column densities of 10^{20} and 10^{22} cm^{-2}.
- For low column densities and low expansion velocities, the profiles are double-peaked with red enhancement, which becomes conspicuous as both the HI column density and expansion velocity increase.
- For large values of v$_{exp}$, a secondary peak and a tertiary peak appear blueward of Hβ, which is attributed to reflection effects that may occur on the interior boundary of the spherical shell.

Raman Conversion Efficiency

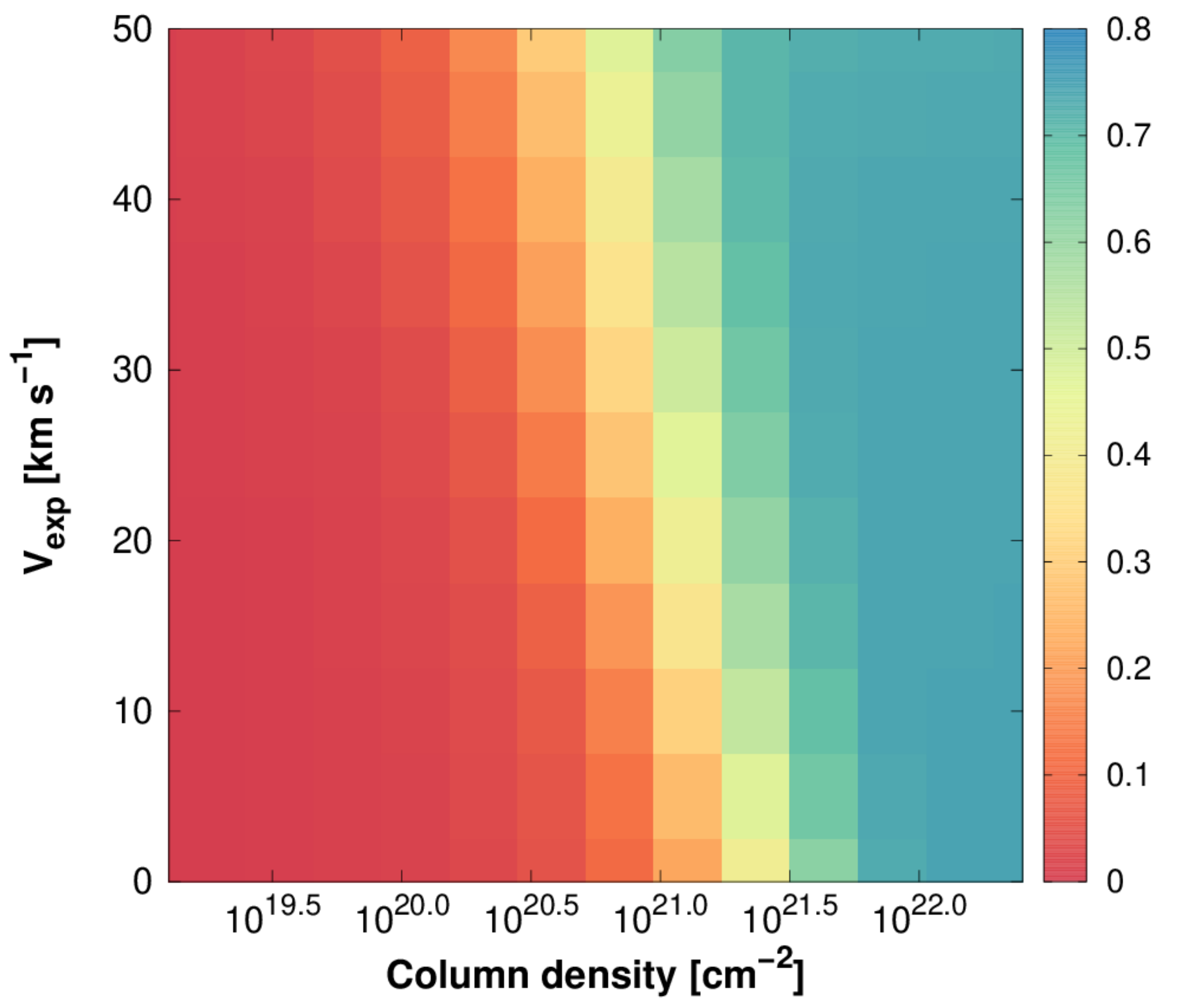

- Conversion efficiency ≡ $\frac{\text{Raman scattered flux}}{\text{The incident far UV flux}}$
- The conversion efficiency tends to increase with N$_{HI}$ and **v$_{exp}$** due to the sharp increase of the cross section.
- The conversion efficiency is saturated at high column density over ~10^{22} cm^{-2}.
- Observationally one may infer the conversion efficiency by measuring the flux ratio of the Raman scattered He II 4850Å and He II 4859 Å line, assuming the validity of the case B recombination theory.

5. Discussion

- Very complicated behaviors including appearance of secondary and tertiary peaks of Raman He II profiles are obtained from a monochromatic line source of He II surrounded by a spherical HI region. Our work will be extended for a point-like He II source with a Gaussian line profile. We expect that Raman line profiles will show redward center-shift and significant profile distortion due to asymmetric cross section.
- Our new code will be also useful to interpret complicated Raman O VI line profiles often exhibited in symbiotic stars, which will shed much light on mass transfer processes in these objects.
- The code is also capable of simulating imaging and spectroscopic polarimetry, which will be useful to investigate the mass loss processes in young planetary nebulae and symbiotic stars.

2019 100th KAS Spring Meeting